*Research Article*

# *In-vitro* Cytotoxicity and *In-silico* Insights of the Multi-target Anticancer Candidates from *Haplophyllum tuberculatum*

**Mosab Yahya Al-Nour** [1]

**Ahmed H. Arbab** [2,3*]

**Mohammad Khalid Parvez** [4]

**Arwa Y. Mohamed** [1]

**Mohammed S. Al-Dosari** [4]

[1]Department of Pharmaceutical Chemistry, Omdurman Islamic University, Omdurman, Sudan

[2]Department of Pharmacognosy, University of Khartoum, Khartoum, Sudan

[3]Department of Pharmacognosy, Omdurman Islamic University, Omdurman, Sudan

[4]Department of Pharmacognosy, King Saud University, Riyadh, Saudi Arabia

*email: arbabssn@gmail.com

## Abstract

This study aimed to investigate the anticancer activity of *Haplophyllum tuberculatum* (Forsk.) aerial parts ethanol extract and fractions and reveal the potential anticancer targets, binding modes, pharmacokinetics, and toxicity properties of its phytoconstituents. MTT assay was used to investigate the anticancer activity. TargetNet, ChemProt version 2.0, and CLC-Pred web servers were used for virtual screening, and Cresset Flare software was used for molecular docking with the 26 predicted targets. Moreover, pkCSM, swiss ADME, and eMolTox web servers were used to predict pharmacokinetics and safety. Ethanolic extracts of *H. tuberculatum* on HepG2 and HeLa cell lines showed promising activities with $IC_{50}$ values 54.12 and 48.1 µg/mL, respectively. Further, ethyl acetate fraction showed the highest cytotoxicity on HepG2 and HeLa cell lines with $IC_{50}$ values 41.7 and 52.31 µg/mL. Of 70 compounds screened virtually, polygamain, justicidin A, justicidin B, haplotubine, kusunokinin, and flindersine were predicted as safe anticancer drugs candidates. They showed the highest binding scores with targets involved in cell growth, proliferation, survival, migration, tumor suppression, induction of apoptosis, metastasis, and drug resistance. Our findings revealed the potency of *H. tuberculatum* as a source of anticancer candidates that further studies should support.

## INTRODUCTION

Cancer is one of the significant health problems in developed and developing countries. It is the second leading cause of death globally[1]. Unfortunately, despite their structural diversity, most currently approved anticancer drugs have drawbacks, mainly due to their harmful effects extended to normal cells, with further consequences on health[2]. Up to date, secondary metabolites continued to be a potential source of anticancer leads and utilized as a source of many therapeutic and preventive anticancer agents. Interestingly, more than 60 % of currently used anticancer drugs are derived from natural sources[3].

*Haplophyllum tuberculatum* (Forsk.) of the Rutaceae family is used in folk medicine for malaria and parasitic infections[4]. Moreover, *H. tuberculatum* is used for many digestive, gynecological, respiratory, cardiovascular, and CNS disorders[5,6]. A literature survey showed that *H.*

*tuberculatum* contains more than 50 phytoconstituents, including polyphenols, alkaloids, lignans, flavonoids, and essential oils[6-10]. Therefore, it is necessary to conduct research to investigate the biological activity, safety, and determination of the appropriate biological target of the phytochemical constituents of *H. tuberculatum.*

Although identifying drug targets is an essential step in understanding the mechanism of action, it is a challenging task mainly because of its complexity. Therefore, there is a need to use advanced technologies such as computer-aided drug design tools, including virtual screening molecular docking, to identify drug targets.[11,12] With this background information, this study aims to investigate the anticancer effect of *H. tuberculatum* aerial parts ethanol extract and fractions on HeLa (cervical) and HepG2 (liver) cell lines, as well as to reveal the potential anticancer targets, binding modes, pharmacokinetics, and toxicity properties of reported phytoconstituents using virtual computational methods.

## MATERIALS AND METHODS

### Materials

Aerial parts (stem, leaves, flowers, fruits) of *H. tuberculatum* were collected from the Southern region of Saudi Arabia. The plant material was authenticated by Dr. Mohammed Yusuf, a taxonomist at the Department of Pharmacognosy, College of Pharmacy, King Saud University, with a voucher specimen (No. 16324) was deposited. Human cancer cell lines HeLa and HepG2 were grown ingrown in T 75 culture flasks (Corning, US) at 37ºC in a humified incubator with 5% $CO_2$ supply. The basic culture medium, DMEM (Invitrogen, US), was supplemented with 10% heat-inactivated bovine serum (Gibco, US) and 1x penicillin-streptomycin (HyClone, US).

### Methods

#### Preparation of ethanol extract and fractions

Dried powdered plant materials (60 g) were soaked in 80% ethanol (Merck, Germany) for three days at 25-30°C and then filtered. Extraction was repeated twice, as described previously. The extract was collected through Whatman filter paper No.1, and then evaporated using a rotary evaporator (Buchi, Switzerland) under reduced pressure at 40°C. The obtained semi-solid extract (5.79 g) was suspended in distilled water and then fractionated three times successively with the same volume of hexane (Merck, Germany), dichloromethane (Merck, Germany), ethyl acetate (Merck, Germany), and aqueous saturated *n*-butanol (Loba Chemie, India) to provide the corresponding fractions. Then, organic solvents were evaporated at reduced pressure using a rotatory evaporator. After drying, ethanol extract and fractions were stored at -20°C until subsequent use for screening.

#### In vitro cytotoxicity assay

Ethanolic extract, as well as fractions of *H. tuberculatum*, were tested for cytotoxic activity using a 3-(4,5-dimethylthiazol-2-yl)-2,5-diphenyltetrazolium bromide (MTT) cell proliferation assay using TACS MTT Cell Proliferation Assay kit (Tervigen, US). The MTT assay was based on the metabolic reduction of soluble MTT by mitochondrial enzyme activity of viable cells into an insoluble colored formazan product which can be solubilized and measured optically[13]. Cells were seeded in flat-bottom 96 well plates ($0.5 \times 10^5$ cells/well) and grown for 20 hours. *Haplophyllum tuberculatum* extract and organic fractions were dissolved in dimethyl sulphoxide (DMSO; 100 mg/mL), then diluted in culture media to prepare five doses (0, 12.5, 25, 50, and 100 µg/mL) of each. The final concentration of DMSO used was less than 0.1%, thus had no toxicity, and cells were treated in triplicate/dose and incubated. Untreated cells (0.1% DMSO in media) and blank (only media) controls

were also included. After 48 hours post-treatment, cells were treated with MTT reagent (10 µL/well) and incubated at 37°C for 4 hours. Upon the appearance of a purple color, the detergent solution (100 µL) was added to each well and further incubated at 37°C for an hour. Optical density (OD) was recorded at 570 nm using a microplate reader ELx800 and cell survival fraction was determined using the equation in **Formula 1**:

$$Survival\ fraction(\%) = \frac{(ODs-ODb)}{(ODc-ODb)} \times 100 \dots [1]$$

In which ODs, ODb, and ODc were the optical density of the sample, blank and negative control, respectively[14]. Data were subjected to analysis using Microsoft Excel software, and the survival fraction was plotted against the concentration. The concentration required for 50% inhibition of cell viability (IC$_{50}$) was calculated. The extracts that fail to inhibit 50% of cell viability up to 100 µg/mL were considered inactive.

*In silico cytotoxicity and drug-likeness prediction*

The cytotoxic effect of about 70 compounds reported *H. tuberculatum* phytochemical constituents[6-10] were predicted using Cell Line Cytotoxicity Predictor (CLC-Pred)[15]. The probability of phytochemical constituents to be a drug candidate was predicted using the SwissADME webserver[16].

*Virtual screening and molecular docking*

Virtual screening for anticancer targets depended on a protocol described by Al-Nour *et al.*[12] with a modification. The chemical structures of reported *H. tuberculatum* phytochemical constituents were sketched by Marven Sketch software version 18.5 and saved as a mol. file format. The 3D structures were generated and optimized accurately using Cresset Flare software[17]. The virtual screening for anticancer targets was conducted by submitting the structures to TargetNet[18], ChemProt version 2.0[19], and CLC-Pred[20] web servers in SMILES format. The predicted targets were for further validation

via molecular docking. The 3D structures of the predicted targets were downloaded from the RCSB protein data bank[21], prepared for docking, and minimized via Cresset Flare software[17]. For the validation, two 3D structures with different PDB IDs were downloaded.

The molecular docking calculations were conducted using Cresset Flare software[17] at the normal mode and default setting. The co-crystallized ligands were used to determine the grid box; however, in the absence of a co-crystallized ligand, the grid box was determined by selecting the active site amino acids. The co-crystallized ligands and the known target's ligands were used as positive controls.

*Pharmacokinetics and toxicity prediction*

The pkCSM[22] and SwissADME[16] web servers were used to predict intestinal absorption, the apparent volume of distribution, clearance, and CYP-450 enzyme inhibition. Furthermore, the pkCSM[22] and eMolTox[20] web servers were used to predict the toxicity of phytochemical constituents on major organs (cardiotoxicity, hepatotoxicity, and renal toxicity).

## RESULTS AND DISCUSSION

*In vitro cytotoxicity assay*

The *in vitro* cytotoxic activity of *H. tuberculatum* ethanol extract and fractions was evaluated against HeLa and HepG2 cancer cell lines. The IC$_{50}$ was calculated by plotting the survival fraction against concentration, as shown in **Figure 1**. *Haplophyllum tuberculatum* ethanol extract showed cytotoxic activity against HeLa and HepG2 with IC$_{50}$ values of 54.12 and 48.1 µg/mL, respectively. In comparison, the IC$_{50}$ values for hexane, chloroform, and ethyl acetate fractions against HeLa cells were 61.12, 79.4, and 52.31 µg/mL, respectively. Only hexane and ethyl acetate fractions showed activity against HepG2 cells with IC$_{50}$ values of 75.6 and 41.7 µg/mL, respectively.
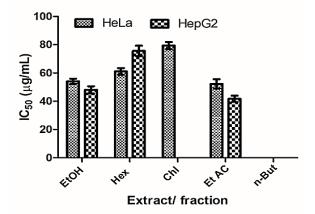
**Figure 1.** *In vitro* cytotoxic activity of the *H. tuberculatum* ethanol extract and fractions against HeLa and HepG2 cell lines by MTT assay; IC$_{50}$, half-maximal inhibitory concentration; EtOH: ethanol extract, Hex: hexane fraction, Chl: chloroform fraction, EtAc: ethyl acetate fraction

These findings revealed that the crude ethanol extract exhibited marked inhibition in both HeLa and HepG2 lines in a dose-dependent manner with IC$_{50}$ values of 54.12 and 48.1 μg/mL, respectively. Therefore, it was subjected to sequential fractionation and subsequent screening. The highest anticancer activity was associated with the ethyl acetate fraction, followed by the hexane fraction (**Figure 1**). Notably, the variable activities shown by the different fractions might be attributed to the diversity of structure and/or uneven distribution of phytochemical constituents present in these fractions. Nevertheless, this further suggests that the bioactive compounds were of low to intermediate polarity.

*Virtual screening and molecular docking*

Once the biological activity was confirmed, identifying the drug target was a valuable subsequent step that leads to further success in the drug development pipeline[11]. It was challenging work; hence, it requires sophisticated tools to reduce the difficulty[12]. Recently, the use of computer-aided drug design tools leads to the successful prediction of many drug targets. Several studies reported the involvement of computational tools in discovering natural drugs[23-26]. Consequently, in this study, virtual screening and molecular docking were used to predict

the targets that phytochemical constituents exert their cytotoxicity through.

Initially, the cytotoxicity and the drug-likeness probability of known phytoconstituents of *H. tuberculatum* were predicted. Out of the 70 screened compounds, 47 were predicted as cytotoxic drug candidates. Their probable targets were predicted, and their interactions were studied using the molecular docking technique. The promised compounds with their target were listed in **Table I**.

According to the virtual screening and molecular docking, the cytotoxic effect of *H. tuberculatum* was due to the interaction with vital targets that were involved in cell growth, proliferation, and survival, migration, tumor suppression, induction of apoptosis, resistance to apoptosis, metastasis, as well as drug resistance. **Table I** shows polygamain, justicidin A, justicidin B, γ-fagarine, skimmianine, haplotubine, kusunokinin, and flindersine were the phytochemical constituents that contribute to the cytotoxicity of *H. tuberculatum*.

Virtual screening was based on strictly evaluated and validated QSAR models[18]. Besides, the molecular docking study was performed using Cresset Flare software characterized by well-respected accuracy and efficiency[17,26]. The predicted cytotoxicity was due to the inhibition of tumor cells growth, proliferation, and survival via the interaction with Dual specificity protein kinase CLK1, Dual specificity tyrosine-phosphorylation-regulated kinase 1A, topoisomerase II enzyme, transcription factor p65, peroxisome proliferator-activated receptor-γ, mitogen-activated protein kinase 14, thyrotropin receptor, and phosphatidylinositol-4 5-bisphosphate 3-kinase catalytic subunit α. Besides, the predicted cytotoxicity was due to tumor suppression via the interaction with Cellular Tumor antigen p53, Menin, Runt-related transcription factor 1, and Serine-protein kinase ATM, as well as the inhibition of tumor cells

migration via the interaction with Tubulin β-2B chain, Receptor-interacting serine/threonine-protein kinase 2, and Protein kinase C αtype. Furthermore, the predicted cytotoxicity was due to the induction of apoptosis via the interaction with Caspase 3 and 8 enzymes tumor necrosis factor receptor superfamily member 6, the inhibition of anti-apoptotic protein Bcl-2 and BAX, as well as the inhibition of drug resistance via the interaction with multidrug resistance protein 1 and 2.

**Table I.** Molecular docking results of the *H. tuberculatum* phytochemical constituents with their predicted targets

| Target | Compounds | Docking score | |
|---|---|---|---|
| Tubulin β-2B chain | | **6E7C** | **5TZ** |
| | Polygamain | -9.925 | -9.175 |
| | Justicidin A | -8.593 | -7.572 |
| | Justicidin B | -9.194 | -8.604 |
| | Haplotubine | -8.127 | -8.555 |
| | Kusunokinin | -8.063 | -8.037 |
| | *A GTP 502* | -9.052 | — |
| | *A GTP 501* | — | -8.672 |
| Dual specificity protein kinase CLK1 | | **1Z57** | **6Q8K** |
| | Polygamain | -9.313 | -9.483 |
| | Justicidin A | -9.098 | -10.163 |
| | Justicidin B | -9.266 | -9.549 |
| | *A DBQ 1* | -8.971 | — |
| | *A FG9 502* | — | -9.332 |
| Dual specificity tyrosine-phosphorylation-regulated kinase 1A | | **6EIJ** | **4NCT** |
| | Polygamain | -8.966 | -9.877 |
| | Dyphylline | -8.004 | -7.942 |
| | Skimmianine | -6.384 | -5.71 |
| | *A B5Z 501* | -10.072 | — |
| | *A 2K2 501* | — | -17.596 |
| Receptor-interacting serine/threonine-protein kinase 2 | | **6C3E** | **4NEU** |
| | Polygamain | -6.408 | -7.675 |
| | Justicidin A | -6.332 | -7.944 |
| | Justicidin B | -7.304 | -7.161 |
| | *A EJY 301* | -7.913 | — |
| | *A Q1A 402* | — | -13.12 |
| Cellular Tumor Antigen p53 | | **6GGA** | **5O1A** |
| | Polygamain | -8.885 | -8.125 |
| | Kusunokinin | -7.831 | -9.274 |
| | Flindersine | -7.194 | -7.935 |
| | *A EY2 401* | -8.323 | — |
| | *A 9H5 402* | — | -8.89 |
| Menin protein | | **4GQ3** | **3U88** |
| | Polygamain | -8.505 | -8.883 |
| | Justicidin A | -8.141 | -8.075 |
| | Justicidin B | -7.901 | -7.878 |
| | Dyphylline | -8.598 | -8.383 |
| | *A 0RO 601* | -9.778 | — |
| | *A 0BR 612* | — | -8.505 |
| Runt-related transcription factor 1 | | **4L0Y** | **1IO4** |
| | Polygamain | -7.563 | -7.313 |
| Caspase 3 enzyme | | **1NMS** | **3EDQ** |
| | Polygamain | -8.628 | -7.764 |
| | Justicidin A | -8.28 | -7.623 |
| | Justicidin B | -9.025 | -8.274 |
| | Dyphylline | -8.738 | -8.376 |
| | Kusunokinin | -8.374 | -7.655 |
| | *A 161 1278* | -9.822 | — |
| | *F ACE 1* | — | -12.374 |
| Topoisomerase II enzyme | | **3QX3** | **5ZAD** |
| | Polygamain | -8.575 | -8.572 |
| | *A EVP 1* | -8.68 | — |
| Multidrug resistance protein 1 and 2 | | **6QEX** | **6FEQ** |
| | Polygamain | -10.035 | -9.3 |
| | *A CLR 1306* | -7.008 | — |
| | *A D6T* | — | -10.498 |
| Topoisomerase I enzyme | | **1TL8** | **1SEU** |
| | Polygamain | -10.996 | -10.555 |
| | Justicidin A | -10.893 | -12.381 |
| | Justicidin B | -9.959 | -11.945 |
| | Dyphylline | -11.278 | -11.976 |
| | Kusunokinin | -10.363 | -10.631 |
| | *D AI3 901* | -12.126 | — |
| | *D SA3 990* | — | -15.519 |
| Caspase 8 enzyme | | **3KJQ** | **1F9E** |
| | Polygamain | -9.995 | -9.777 |
| | Justicidin A | -9.545 | -7.023 |
| | Justicidin B | -8.736 | -7.959 |
| | Dyphylline | -9.07 | -7.448 |
| | *A B94 480* | -10.132 | — |
| Transcription factor p65 | | **2RAM** | **5U01** |
| | P-cymene-8-ol | -5.597 | -5.766 |
| | Justicidin A | -6.821 | -7.159 |
| | Justicidin B | -7.221 | -8.214 |
| | **Bortezomib** | -6.232 | -6.29 |
| Protein kinase C α type | | **4DNL** | **3IW4** |
| | Justicidin A | -7.37 | -8.928 |
| | Justicidin B | -7.48 | -8.928 |
| | Dyphylline | -7.442 | -10.394 |
| | *A LW4 901* | — | -12.252 |
| Peroxisome proliferator-activated receptor γ | | **4CI4** | **6MS7** |
| | Justicidin A | -8.329 | -8.421 |
| | Justicidin B | -9.245 | -8.781 |
| | Dyphylline | -9.801 | -6.78 |
| | *A Y1N 1468* | -10.537 | — |
| | *A V77 601* | — | -7.283 |
| Receptor tyrosine-protein kinase erbB-2 | | **2A91** | **3BE1** |
| | Justicidin A | -7.344 | -9.024 |
| | Justicidin B | -8.243 | -8.799 |
| | Dyphylline | -7.711 | -9.223 |
| Mitogen-activated protein kinase 14 | | **3U8W** | **3GFE** |
| | γ-fagarine | -11.738 | -6.368 |
| | *A 09J 500* | -11.738 | — |
| | *A P37 361* | — | -12.126 |
| Thyrotropin receptor | | **2XWT** | **3G04** |
| | γ-fagarine | -6.029 | -6.126 |
| | Skimmianine | -6.319 | -6.172 |
| | Kusunokinin | -7.016 | -6.961 |
| | Flindersine | -6.657 | -7.058 |
| Phosphatidylinositol-4 5-bisphosphate 3-kinase catalytic subunit α | | **5XGH** | **6GVF** |
| | γ-fagarine | -6.74 | -6.117 |
| | Skimmianine | -6.605 | -7.031 |
| Serine-protein kinase ATM | | **6FH5** | **3JBZ** |
| | Skimmianine | -7.356 | -6.257 |
| | *A ADP 2601* | -9.672 | — |
| | | — | -10.074 |
| Tumor necrosis factor receptor superfamily member 6 | | **3OQ9** | **3THM** |
| | γ-fagarine | -7.234 | -5.852 |
| | Skimmianine | -7.305 | -5.748 |
| | Kusunokinin | -7.172 | -7.294 |
| | Flindersine | -7.936 | -7.429 |
| Apoptosis regulator Bcl-2 | | **2VM6** | **5WHH** |
| | Haplotubine | -8.216 | -6.934 |
| | Kusunokinin | -7.08 | -6.257 |
| | Flindersine | -7.055 | -7.116 |
| | **Venetoclax** | -9.339 | -8.807 |
| Apoptosis regulator BAX | | **5W5X** | **6EB6** |
| | Flindersine | -6.726 | -6.87 |

Note: The bolded code was the target 3D structure were the PDB IDs. The italic compounds were the co-crystallized ligands. The bolded compounds were positive controls

According to molecular docking, the lowest energy score indicates the highest binding affinity[27]. Hence, polygamain, justicidin A, justicidin B, haplotubine, kusunokinin, and flindersine were the compounds with the highest binding affinity. The 3D interaction of the best-predicted compounds shows a ligand superimposing between the best-predicted compounds and the controls. However, polygamain binds at a different position on the active site of the multidrug resistance protein 1 from the co-crystallized ligand A CLR 1306, as shown in **Figure 2**. Polygamain has the highest binding affinity to the vast majority of the predicted targets among the best-predicted compounds. Due to the vast number of predicted targets, a representative example was given to illustrate the 3D and 2D interactions. The results showed that polygamain interacts with the Dual specificity tyrosine-phosphorylation-regulated kinase 1A and Cellular Tumor antigen p53 in the same binding sites of their co-crystallized ligands. It binds with the exact position of A B5Z 501 and a different position from A EY2 401. In contrast, justicidin A binds in a position similar to D SA3 990, as shown in **Figure 2**.

In comparison between interactions of polygamain, justicidin A, and the co-crystallized ligands, A B5Z 501 forms additional hydrogen bond with the dual specificity tyrosine-phosphorylation-regulated kinase 1A binding site making its virtual screening score (-10.072) better than polygamain (-8.966). The A EY2 401 forms six hydrophobic bonds with the binding sites of the Cellular Tumor antigen p53, much than polygamain (three bonds). However, the amino acids clashes made its virtual screening score (-8.323) lower than polygamain (-8.885). In contrast, the atom clashes and fewer bonds in the interaction of justicidin A with the topoisomerase I enzyme made its virtual screening score (-10.893) lower than D SA3 990 (-15.519), as shown in **Figure 3**.
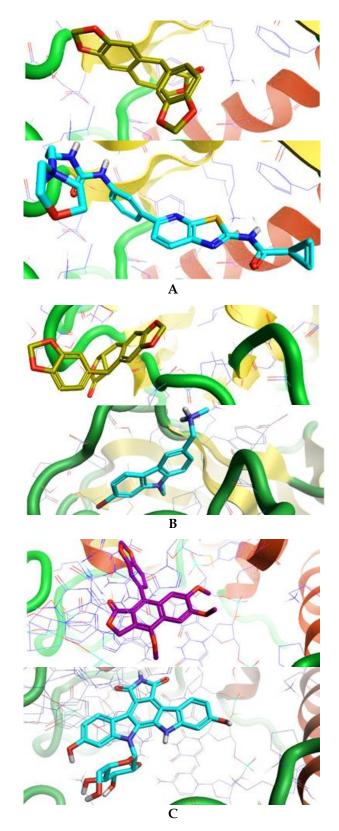


**Figure 2.** The 3D interaction between the best predicted *H. tuberculatum* phytochemical constituents with their predicted targets. **A**: Polygamain (**dark yellow**) and A B5Z 501 (**turquoise**) with dual-specificity tyrosine phosphorylation-regulated kinase 1A. **B**: Polygamain (**dark yellow**) and A EY2 401 (**turquoise**) with Cellular Tumor antigen p53. **C**: Justicidin A (**violet**) and D SA3 990 (**turquoise**) with Topoisomerase I enzyme.
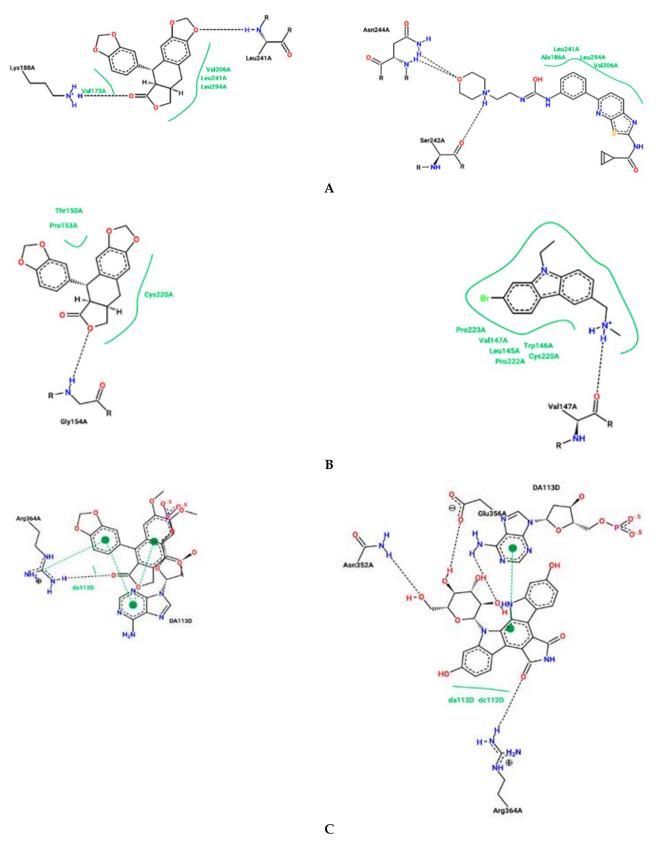
**Figure 3.** The 2D interaction between the best predicted *H. tuberculatum* phytochemical constituents with their predicted targets. **A**: Polygamain (**left**) and A B5Z 501 (**right**) with dual-specificity tyrosine phosphorylation-regulated kinase 1A. **B**: Polygamain (**left**) and A EY2 401 (**right**) with Cellular Tumor antigen p53. **C**: Justicidin A (**left**) and D SA3 990 (**right**) with Topoisomerase I enzyme.

*Pharmacokinetics and toxicity prediction*

Web servers were used to predict the promised anticancer phytochemical constituents of *H. tuberculatum* compounds' toxicity, and results are summarized in Table II. Polygamain, skimmianine, kusunokinin, and flindersine had the best pharmacokinetics and safety profile among those compounds. Moreover, the pharmacokinetics and toxicity prediction results of polygamain showed that it had the highest absorption (100%), was permeable to the blood-brain-barrier BBB, and was free from significant organ toxicity (cardiotoxicity hepatotoxicity, nephrotoxicity, and CNS toxicity). Consequently, polygamain would be a promising drug-like compound for the treatment of many types of cancers.

**Table II.** Pharmacokinetics and toxicity prediction of the promising *H. tuberculatum* phytochemical constituents

| Compounds | GIT absorption | BBB* | Vd** | Cl*** | CYP450 enzymes inhibition | Toxicity on major organs |
|---|---|---|---|---|---|---|
| Polygamain | High (100%) | Yes | -0.855 | -0.042 | CYP3A4, CYP1A2 | No |
| Ammoidin | High (98.341) | Yes | -0.198 | 0.744 | CYP1A2 | No |
| Skimmianine | High (97.967) | Yes | 0.046 | 0.757 | CYP3A4, CYP1A2 | No |
| Kusunokinin | High (97.192) | Yes | -0.435 | 0.115 | CYP3A4, CYP2C19, CYP2C9 | No |
| Flindersine | High (95.319) | Yes | 0.543 | 0.196 | CYP1A2 | No |

*Blood brain barrier permeability, **Volume of distribution (-log/Kg), ***Clearance (log mL/min/kg)

In agreement, polygamain from *Amyris madrensis* was found to has a cytotoxic effect against human PC3 cells[28]. Justicidin B was found to had a potent cytotoxic and pro-apoptotic effect on human breast cancer-derived cell lines[29] and acute myeloid leukemia-derived cell line HL-60[30]. Though the effectiveness of using virtual screening and molecular docking for drug targets prediction[12,17,18], experimental studies were recommended to validate the predicted targets to develop strong evidence regarding the role of the predicted target in the cytotoxicity of *H.*

*tuberculatum* phytochemical constituents. Moreover, RMSD calculations and molecular dynamics simulation are recommended to validate docking calculations.

## CONCLUSION

Our findings concluded that *H. tuberculatum* has anticancer potential. Polygamain, justicidin A, justicidin B, γ-fagarine, skimmianine, haplotubine, kusunokinin, and flindersine were the phytochemical constituents that contribute to the cytotoxicity of *H. tuberculatum*. They exert their cytotoxic effect via the interaction with vital targets involved in cell growth, proliferation, and survival, migration, tumor suppression, induction of apoptosis, resistance to apoptosis, metastasis, as well as drug resistance. However, further phytochemical and biological studies are required to isolate the active principle(s) responsible for the novel anticancer potential.

## ACKNOWLEDGMENT

None.

## AUTHORS' CONTRIBUTION

**Mosab Yahya Al-Nour**: conceptualization, molecular docking, data entry and analysis. **Ahmed H. Arbab**: supervision, extraction, MTT assay, data analysis. **Mohammad Khalid Parvez**: conceptualization, MTT assay, supervision. **Arwa Y. Mohamed**: molecular docking, data analysis. **Mohammed S. Al-Dosari**: supervision, conceptualization, MTT assay.

## DATA AVAILABILITY

None.

## CONFLICT OF INTEREST

The authors declare no conflict of interest.

## REFERENCES

1. Nagai H, Kim YH. Cancer prevention from the perspective of global cancer burden patterns. J Thorac Dis. 2017;9(3):448-51. doi:10.21037/jtd.2017.02.75

2. Nurgali K, Jagoe RT, Abalo R. Editorial: Adverse Effects of Cancer Chemotherapy: Anything New to Improve Tolerance and Reduce Sequelae? Front Pharmacol. 2018;9:245. doi:10.3389/fphar.2018.00245

3. Rayan A, Raiyn J, Falah M. Nature is the best source of anticancer drugs: Indexing natural products for their anticancer bioactivity. PLoS One. 2017;12(11):e0187925. doi:10.1371/journal.pone.0187925

4. Hamdi A, Bero J, Beaufay C, Flamini G, Marzouk Z, Heyden YV, et al. In vitro antileishmanial and cytotoxicity activities of essential oils from Haplophyllum tuberculatum A. Juss leaves, stems and aerial parts. BMC Complement Altern Med. 2018;18(1):60. doi:10.1186/s12906-018-2128-6

5. Eissa TF, González-Burgos E, Carretero ME, Gómez-Serranillos MP. Biological activity of HPLC-characterized ethanol extract from the aerial parts of Haplophyllum tuberculatum. Pharm Biol. 2014;52(5):151-6. doi:10.3109/13880209.2013.819517

6. Al-Snafi AE. Pharmacological importance of Haplophyllum species grown in Iraq- A review. IOSR J Pharm. 2018;8(5):54-62.

7. Al-Rehaily AJ, Al-Howiriny TA, Ahmad MS, Al-Yahya MA, El-Feraly FS, Hufford CD, et al. Alkaloids from Haplophyllum tuberculatum. Phytochemistry. 2001;57(4):597-602. doi:10.1016/s0031-9422(01)00041-3

8. Sheriha GM, Amer KMA. Lignans of haplophyllum tuberculatum. Phytochemistry. 1984;23(1):151-3. doi:10.1016/0031-9422(84)83096-4

9. Aberrane A, Djouahri A, Djerrad Z, Saka B, Benseradj F, Aitmoussa S, et al. Changes in essential oil composition of Haplophyllum tuberculatum (Forssk.) A. Juss. aerial parts according to the developmental stage of growth and incidence on the biological activities. J Essent Oil Res. 2019;31(1):69-89. doi:10.1080/10412905.2018.1511483

10. Khalid SA, Waterman PG. Alkaloid, lignan and flavonoid constituents of Haplophyllum tuberculatum from Sudan. Planta Med. 1981;43(2):148-52. doi:10.1055/s-2007-971491

11. Jones LH. An industry perspective on drug target validation. Expert Opin Drug Discov. 2016;11(7):623-5. doi:10.1080/17460441.2016.1182484

12. Al-Nour MY, Ibrahim MM, Elsaman T. Ellagic Acid, Kaempferol, and Quercetin from Acacia nilotica: Promising Combined Drug With Multiple Mechanisms of Action. Curr Pharmacol Rep. 2019;5:255-80. doi:10.1007/s40495-019-00181-w

13. Kumar P, Nagarajan A, Uchil PD. Analysis of Cell Viability by the MTT Assay. Cold Spring Harb Protoc. 2018;2018(6). doi:10.1101/pdb.prot095505

14. Arbab AH, Parvez MK, Al-Dosari MS, Al-Rehaily AJ, Ibrahim KE, Alam P, et al. Therapeutic efficacy of ethanolic extract of Aerva javanica aerial parts in the amelioration of CCl4-induced hepatotoxicity and oxidative damage in rats. Food Nutr Res. 2016;60:30864. doi:10.3402/fnr.v60.30864

15. Lagunin A, Stepanchikova A, Filimonov D, Poroikov V. PASS: prediction of activity spectra for biologically active substances. Bioinformatics. 2000;16(8):747-8. doi:10.1093/bioinformatics/16.8.747

16. Daina A, Michielin O, Zoete V. SwissADME: a free web tool to evaluate pharmacokinetics, drug-likeness and medicinal chemistry friendliness of small molecules. Sci Rep. 2017;7:42717. doi:10.1038/srep42717

17. Cheeseright T, Mackey M, Rose S, Vinter A. Molecular field extrema as descriptors of biological activity: definition and validation. J Chem Inf Model. 2006;46(2):665-76. doi:10.1021/ci050357s

18. Yao ZJ, Dong J, Che YJ, Zhu MF, Wen M, Wang NN, et al. TargetNet: a web service for predicting potential drug-target interaction profiling via multi-target SAR models. J Comput Aided Mol Des. 2016;30(5):413-24. doi:10.1007/s10822-016-9915-2

19. Kjærulff SK, Wich L, Kringelum J, Jacobsen UP, Kouskoumvekaki I, Audouze K, et al. ChemProt-2.0: visual navigation in a disease chemical biology database. Nucleic Acids Res. 2013;41(Database issue):D464-9. doi:10.1093/nar/gks1166

20. Lagunin AA, Dubovskaja VI, Rudik AV, Pogodin PV, Druzhilovskiy DS, Gloriozova TA, et al. CLC-Pred: A freely available web-service for in silico prediction of human cell line cytotoxicity for drug-like compounds. PLoS One. 2018;13(1):e0191838. doi:10.1371/journal.pone.0191838

21. Bernstein FC, Koetzle TF, Williams GJ, Meyer Jr EF, Brice MD, Rodgers JR, et al. The Protein Data Bank: a computer-based archival file for macromolecular structures. J Mol Biol. 1977;112(3):535-42. doi:10.1016/s0022-2836(77)80200-3

22. Pires DEV, Blundell TL, Ascher DB. pkCSM: Predicting Small-Molecule Pharmacokinetic and Toxicity Properties Using Graph-Based Signatures. J Med Chem. 2015;58(9):4066-72. doi:10.1021/acs.jmedchem.5b00104

23. Mahajan P, Wadhwa B, Barik MR, Malik F, Nargotra A. Combining ligand- and structure-based in silico methods for the identification of natural product-based inhibitors of Akt1. Mol Divers. 2020;24(1):45-60. doi:10.1007/s11030-019-09924-9

24. Pereira F, Aires-de-Sousa J. Computational Methodologies in the Exploration of Marine Natural Product Leads. Mar Drugs. 2018;16(7):236. doi:10.3390/md16070236

25. Prachayasittikul V, Worachartcheewan A, Shoombuatong W, Songtawee N, Simeon S, Prachayasittikul V, et al. Computer-Aided Drug Design of Bioactive Natural Products. Curr Top Med Chem. 2015;15(18):1780-800. doi:10.2174/1568026615666150506151101

26. Ibrahim MM, Elsaman T, Al-Nour MY. Synthesis, Anti-Inflammatory Activity, and In Silico Study of Novel Diclofenac and Isatin Conjugates. Int J Med Chem. 2018;2018:9139786. doi:10.1155/2018/9139786

27. Pantsar T, Poso A. Binding Affinity via Docking: Fact and Fiction. Molecules. 2018;23(8):1899. doi:10.3390/molecules23081899

28. Peng J, Hartley RM, Fest GA, Mooberry SL. Amyrisins A-C, O-prenylated flavonoids from Amyris madrensis. J Nat Prod. 2012;75(3):494-6. doi:10.1021/np200796e

29. Momekov G, Konstantinov S, Dineva I, Ionkova I. Effect of justicidin B - a potent cytotoxic and pro-apoptotic arylnaphtalene lignan on human breast cancer-derived cell lines. Neoplasma. 2011;58(4):320-5. doi:10.4149/neo_2011_04_320

30. Momekov G, Yossifov D, Guenova M, Michova A, Stoyanov N, Konstantinov S, et al. Apoptotic mechanisms of the biotechnologically produced arylnaphtalene lignan justicidin B in the acute myeloid leukemia-derived cell line HL-60. Pharmacol Rep. 2014;66(6):1073-6. doi:10.1016/j.pharep.2014.07.005